Hamiltonian Truncation Revisited

J. Ingoldby

Durham University, IPPP

August 12th, 2024

Outline

Method Overview

Hamiltonian Setup

$$H = H_0 + V \tag{1}$$

- H_0 is an exactly solvable Hamiltonian
- V represents a new interaction, which may be strong.
- Work in the eigenbasis of H_0. Truncate so that only a finite number of states with $E_0 \leq E_T$ are included in the basis.
- Diagonalize numerically to calculate spectrum and wavefunctions.

A Simple Example: The Anharmonic Oscillator

Take the quantum mechanical model

$$H = \frac{p^2 + x^2}{2} + \lambda x^4 . \tag{2}$$

Decompose the Hamiltonian so that H_0 is the SHO and $V = \lambda x^4$. Work in the SHO eigenbasis: $H_0 |n\rangle = (n + 1/2) |n\rangle$

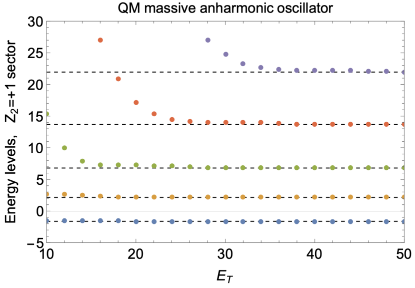

- Truncate basis to include states $|n\rangle$ for $n + 1/2 \leq E_T$.
- All energy eigenvalues are upper bounds for the true energies due to min-max theorem.
- Method generalises to QFTs.

What QFTs Have Been Studied Using HT?

An incomplete selection of studies, with an hep-th focus: Please see [Konik et al '17], [Katz, Fitzpatrick '22] for a more complete review.

In 2 dimensions

- Minimal model CFT deformed with relevant primary operator [Yurov, Zamolodchikov '89]...
- $\mathrm{SU}(3)$ gauge theory with fundamental Dirac fermions on the lightcone [Hornbostel, Brodsky, Pauli '90]...
- ϕ^4 deformation of massive scalar field [Rychkov, Vitale '14], [Cohen, Farnsworth, Houtz, Luty '21] ...

What QFTs Have Been Studied Using HT?

An incomplete selection of studies, with an hep-th focus: Please see [Konik et al '17], [Katz, Fitzpatrick '22] for a more complete review.

In 3 dimensions

- $\phi^2 + i\phi^3$ deformation of free scalar CFT on S^3 [Hogervorst '18]...
- ϕ^4 deformation of massive scalar on $\mathbb{R} \times T^2$ [Elias-Miró, Hardy '18]...
- ϕ^4 deformation of scalar CFT on the lightcone [Anand, Katz, Khandker, Walters '18]...

Truncated Conformal Space Approach

[Yurov, Zamolodchikov '89], [Lassig, Mussardo, Cardy '90], ..., [Hogervorst, Rychkov, van Rees '14], ...

QFTs can very generally be realized as RG flows between a pair of CFTs.

$$H = H_{\text{CFT}} + V_{\Delta} \tag{3}$$

Put UV CFT onto the cylinder $\mathbb{R} \times S^R_{d-1}$:

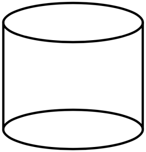

The dilatation operator on the plane $\mathbb{R}^d$ gets Weyl mapped to the time translation generator on the cylinder: $D \to H$

Truncated Conformal Space Approach

Take V_Δ to be the space integral of a local relevant operator

$$V_\Delta = gR^{\Delta - d} \int_{S_R^{d-1}} d^{d-1}x \, \phi_\Delta(x) \,. \tag{4}$$

The matrix elements of V_Δ between states $\langle \Delta_i |$ and $| \Delta_j \rangle$ are given by OPE coefficients $C_{i\phi j}$. The full Hamiltonian becomes:

$$H_{ij} = \frac{1}{R} \left(\Delta_i \delta_{ij} + g C_{i\phi j} \right) \tag{5}$$

- Truncate to retain states $\Delta_i < \Delta_T$.
- Diagonalizing H gives *finite volume* spectrum.
- TCSA can be used even at strong coupling $g \gtrsim 1$.
- Lightcone Conformal Truncation is an interesting alternative e.g. [Katz et al '20].

Extrapolating to the "Continuum Limit"

Just like in a lattice calculation, to make contact with the original QFT, you need to numerically extrapolate TCSA results to the continuum limit. In our case, this corresponds to taking $\Delta_T \to \infty$ and $R \to \infty$.

Extrapolating to the "Continuum Limit"

Just like in a lattice calculation, to make contact with the original QFT, you need to numerically extrapolate TCSA results to the continuum limit. In our case, this corresponds to taking $\Delta_T \to \infty$ and $R \to \infty$.

For d-dimensional CFTs, the number of states grows exponentially with scaling dimension [Cardy '91]:

$$N(\Delta) \sim \exp\{\alpha \Delta^{\frac{d-1}{d}}\}\,. \tag{6}$$

Therefore the size of the TCSA Hilbert space will also grow exponentially with Δ_T.

Exponential Scaling

In a QFT without UV divergences, the error in a typical HT calculation tends to scale in a power like way with the cutoff $\epsilon \sim E_T^{-b}$ as you approach the continuum limit.

The cost of a HT calculation grows exponentially with the tolerance

$$\dim \mathcal{H}_T \sim \exp\{1/\epsilon^{\text{const}}\}\,. \tag{7}$$

Exponential Scaling

In a QFT without UV divergences, the error in a typical HT calculation tends to scale in a power like way with the cutoff $\epsilon \sim E_T^{-b}$ as you approach the continuum limit.

The cost of a HT calculation grows exponentially with the tolerance

$$\dim \mathcal{H}_T \sim \exp\{1/\epsilon^{\text{const}}\}\,. \tag{7}$$

1. Despite the exponential scaling, useful precision can be obtained with readily available computing resources.

Exponential Scaling

In a QFT without UV divergences, the error in a typical HT calculation tends to scale in a power like way with the cutoff $\epsilon \sim E_T^{-b}$ as you approach the continuum limit.

The cost of a HT calculation grows exponentially with the tolerance

$$\dim \mathcal{H}_T \sim \exp\{1/\epsilon^{\text{const}}\}\,. \tag{7}$$

1. Despite the exponential scaling, useful precision can be obtained with readily available computing resources.
2. Quantum Computing promises to enable calculation in an exponentially big truncated Hilbert space using polynomial resources.

Exponential Scaling

In a QFT without UV divergences, the error in a typical HT calculation tends to scale in a power like way with the cutoff $\epsilon \sim E_T^{-b}$ as you approach the continuum limit.

The cost of a HT calculation grows exponentially with the tolerance

$$\dim \mathcal{H}_T \sim \exp\{1/\epsilon^{\text{const}}\}\,. \tag{7}$$

1. Despite the exponential scaling, useful precision can be obtained with readily available computing resources.
2. Quantum Computing promises to enable calculation in an exponentially big truncated Hilbert space using polynomial resources.
3. Heuristically, this is because n_q entangled qubits can represent a Hilbert space of dimension 2^{n_q}.

UV Divergences in HT

Based on:

1. [J. Elias-Miró and J. I '22]
2. [J. Elias-Miró, J. I and O. Delouche '24]

UV Divergences

Unfortunately, TCSA calculations are not guaranteed to converge to any finite value as $\Delta_T \to \infty$ when there are UV divergences.

UV Divergences

Unfortunately, TCSA calculations are not guaranteed to converge to any finite value as $\Delta_T \to \infty$ when there are UV divergences.

- No UV divs for $\Delta < d/2$. TCSA works straightforwardly here.

UV Divergences

Unfortunately, TCSA calculations are not guaranteed to converge to any finite value as $\Delta_T \to \infty$ when there are UV divergences.

- No UV divs for $\Delta < d/2$. TCSA works straightforwardly here.
- More subtle when $d > \Delta \geq d/2$. The full QFT has UV divergences in perturbation theory and requires renormalization.

UV Divergences

Unfortunately, TCSA calculations are not guaranteed to converge to any finite value as $\Delta_T \to \infty$ when there are UV divergences.

- No UV divs for $\Delta < d/2$. TCSA works straightforwardly here.
- More subtle when $d > \Delta \geq d/2$. The full QFT has UV divergences in perturbation theory and requires renormalization.
- The TCSA cutoff may be viewed as an awkward, nonlocal UV regulator. UV divergences show up as infinities in the limit $\Delta_T \to \infty$.

UV Divergences

Unfortunately, TCSA calculations are not guaranteed to converge to any finite value as $\Delta_T \to \infty$ when there are UV divergences.

- No UV divs for $\Delta < d/2$. TCSA works straightforwardly here.
- More subtle when $d > \Delta \geq d/2$. The full QFT has UV divergences in perturbation theory and requires renormalization.
- The TCSA cutoff may be viewed as an awkward, nonlocal UV regulator. UV divergences show up as infinities in the limit $\Delta_T \to \infty$.
- Want to extend TCSA to calculate reliably when $d > \Delta \geq d/2$. This is not straightforward due to unusual properties of the TCSA regulator. This is the problem I will focus on in this section!

Relevance

Two very interesting strongly interacting QFTs can be realized as relevant deformations of a UV CFT with $d > \Delta \geq d/2$:

QED$_3$

Flows to an interacting CFT in the IR for $N_f \gtrsim 4$ (4 component ψ).

$$H = H_{\text{CFT}} + m \int d^3x \sum_i \bar{\psi}_i \psi_i$$

$$\Delta_{\bar{\psi}\psi} \sim 2, \quad d/2 = 1.5$$

QCD$_4$

Flows to an interacting CFT in the IR for $33/2 > N_f \gtrsim 9$ for $N_c = 3$.

$$H = H_{\text{BZ}} + m \int d^4x \sum_i \bar{\psi}_i \psi_i$$

$$\Delta_{\bar{\psi}\psi} \sim 3, \quad d/2 = 2$$

Sharpening the Problem with PT

We analyze UV divergences in the lowest few orders in perturbation theory using two regulators:

1. Rayleigh Schrödinger PT with TCSA regulator

$$E_i\, R = \Delta_i + V_{ii} + V_{ik} \frac{1}{\Delta_{ik}} V_{ki} + \dots \tag{8}$$

2. Conformal PT with a local regulator

$$E_{gs}\, R = -\frac{g^2 S_{d-1}}{2!} \int d^d x |x|^{\Delta - d} \langle \phi_\Delta(x) \phi_\Delta(1) \rangle + \dots \tag{9}$$

Check whether the two formulations of PT give consistent results.

Summary of Results

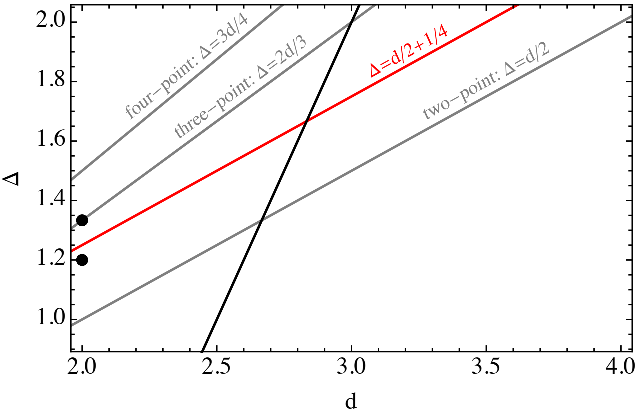

New UV divergences appear in HT that do not if a local regulator is used. This suggests that nonlocal counterterms are essential for renormalization.

Effective Hamiltonians

We can take an effective Hamiltonian (see [Cohen, Farnsworth, Houtz, Luty '21]) and apply it in the case of a QFT with UV divergences:

Effective Hamiltonians

We can take an effective Hamiltonian (see [Cohen, Farnsworth, Houtz, Luty '21]) and apply it in the case of a QFT with UV divergences:

1. First use a local regulator (ϵ) to remove UV divergences from integrated, connected correlation functions

$$E_{gs}^{(n)} R \propto g^n \int_\epsilon \prod_{i=1}^{n-1} d^d x_i |x_i|^{\Delta - d} \langle \phi_\Delta(1) \phi_\Delta(x_1) \ldots \phi_\Delta(x_{n-1}) \rangle_{\text{conn}}$$

and add local counterterms to the full theory Hamiltonian as needed to make the $\epsilon \to 0$ limit well defined

$$H(\epsilon) = H_0 + gV + H_{ct}(\epsilon)$$

This implements local renormalization.

Procedure for Handling UV Divergences

2. Calculate finite dimensional H_{eff} in this renormalized theory in PT.

$$H_{\text{eff}}(\epsilon)_{ij} = H(\epsilon)_{ij} + \sum_{n>2} H_{\text{eff n}}(\epsilon)\,, \tag{10}$$

where $H_{\text{eff n}}$ is $O(g^n)$. Compute as many orders as you need to ensure all matrix elements are finite as $\epsilon \to 0$.

Procedure for Handling UV Divergences

2. Calculate finite dimensional H_{eff} in this renormalized theory in PT.

$$H_{\text{eff}}(\epsilon)_{ij} = H(\epsilon)_{ij} + \sum_{n>2} H_{\text{eff n}}(\epsilon)\,, \tag{10}$$

   where $H_{\text{eff n}}$ is $O(g^n)$. Compute as many orders as you need to ensure all matrix elements are finite as $\epsilon \to 0$.

3. Take the $\epsilon \to 0$ limit analytically for fixed Δ_T

$$H_{\text{eff}} = H_0 + gV + K \tag{11}$$

   The bit left over, K, will in general grow with Δ_T and be *nonlocal*.

Computation at Second Order

Write $H_{eff\,2}$ as an integral of a correlation function:

$$
\begin{aligned}
\left(H_{eff\,2}(\epsilon)\right)_{fi} &= \frac{V_{fh}V_{hi}}{E_{ih}}\,, \\
&= -\frac{g^2 S_{d-1}}{2R} \int\limits_{\substack{0\le|x|<1 \\ |1-x|>\epsilon}} d^d x |x|^{\Delta-d} \left\langle f \right| \phi_\Delta(1) \vdots \phi_\Delta(x) \left| i \right\rangle \,,
\end{aligned}
$$

where we have inserted a partial resolution of the identity

$$
\vdots \equiv \sum \left| h \right\rangle \left\langle h \right| \,.
$$

Computation at Second Order

The integral is over the red region below (minus an ϵ–ball)

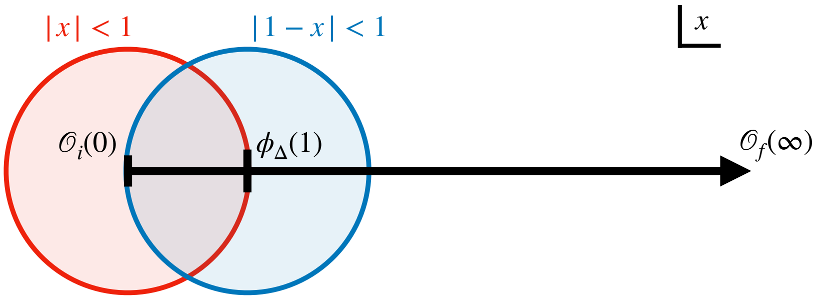

In the blue region, we can use the OPE for $\phi_\Delta(1)\phi_\Delta(x)$

$$\langle f|\,\phi_\Delta(1)\phi_\Delta(x)\,|i\rangle = \sum_{\mathcal{O}} \langle \mathcal{O}_f(\infty)\mathcal{O}(1)\mathcal{O}_i(0)\rangle \, \langle \mathcal{O}(\infty)\phi_\Delta(1)\phi_\Delta(x)\rangle \,,$$

Computation at Second Order

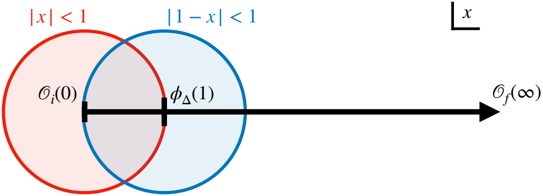

We can neglect the second term below. It is independent of ϵ and will converge to something finite as $\Delta_T \to \infty$.

$$(H_{\text{eff }2}(\epsilon))_{fi} = -\frac{g^2 S_{d-1}}{2R} \sum_{\mathcal{O}} \langle f | \mathcal{O}(1) | i \rangle \int\limits_{\substack{0 \leq |x| < 1 \\ 1 > |1-x| > \epsilon}} d^d x |x|^{\Delta - d} \langle \mathcal{O}(\infty) \phi_\Delta(1) \mid \phi_\Delta(x) \rangle$$

$$- \frac{g^2 S_{d-1}}{2R} \int\limits_{\substack{0 \leq |x| < 1 \\ |1-x| \geq 1}} d^d x |x|^{\Delta - d} \langle f | \phi_\Delta(1) \mid \phi_\Delta(x) | i \rangle \ .$$

Computation at Second Order

For primary scalars

$$\langle \mathcal{O}(\infty)\phi_\Delta(1)\phi_\Delta(x)\rangle = \frac{f_{\mathcal{O}\phi\phi}}{|1-x|^{2\Delta-\Delta_{\mathcal{O}}}} = f_{\mathcal{O}\phi\phi}\sum_{n=0}^{\infty}|x|^n\, C_n^{(2\Delta-\Delta_{\mathcal{O}})/2}(\cos\theta)\,,$$

and we can integrate each term in the series expansion separately

$$u_n^{\Delta',\epsilon} \equiv (2n+\Delta)\int_{\substack{0\le|x|<1\\|1-x|>\epsilon}} d^d x|x|^{2n+\Delta-d}\, C_n^{\Delta'/2}(\cos\theta)\,,$$

$$(H_{\mathrm{eff}\ 2}(\epsilon))_{fi} = -\frac{g^2 S_{d-1}}{2R}\sum_{\mathcal{O}}\langle f|\,\mathcal{O}(1)\,|i\rangle\, f_{\mathcal{O}\phi\phi}\sum_{2n+\Delta>\Delta_T-\Delta_i}^{\infty}\frac{u_n^{2\Delta-\Delta_{\mathcal{O}},\epsilon}}{2n+\Delta} + \text{finite}$$

Scheme Choice

We choose to add the following counterterms, which make $H_{eff,2}$ finite in the $\epsilon \to 0$ limit:

$$H_0 + V \to H_0 + V + \sum_{2\Delta - \Delta_{\mathcal{O}} - d \geq 0} \left(\lambda^{\mathcal{O}}(\epsilon) + \lambda^{\mathcal{O}}_{ren}\right) \int_{S_{d-1}} d^{d-1}x \, \mathcal{O}(x) \, ,$$

$$\lambda^{\mathcal{O}}_{\text{ct}}(\epsilon) \equiv \frac{g^2}{2R} \int_{\substack{0 \leq |x| < 1 \\ 1 > |1-x| > \epsilon}} d^d x |x|^{\Delta - d} \langle \mathcal{O}(\infty) \phi_\Delta(1) \phi_\Delta(x) \rangle \, , \tag{12}$$

$$\lambda^{\mathcal{O}}_{\text{ct}}(\epsilon) = \frac{g^2 f_{\phi\phi\mathcal{O}}}{2R} \sum_{n=0}^{\infty} \frac{u_n^{2\Delta - \Delta_{\mathcal{O}}, \epsilon}}{2n + \Delta} \, .$$

Result at Second Order

Renormalized Effective Hamiltonian

$$K_2 = S_{d-1} \sum_{\Delta_{\mathcal{O}} < 2\Delta - d} \langle f | \, \mathcal{O}(1) \, | i \rangle \left(\lambda^{\mathcal{O}}_{\text{ren}} + \frac{g^2 f_{\phi\phi\mathcal{O}}}{2} \sum_{n=0}^{2n+\Delta \leq \Delta_T - \Delta_i} \frac{u_n^{2\Delta - \Delta_{\mathcal{O}}}}{2n + \Delta} \right) + \dots \tag{13}$$

Result at Second Order

Renormalized Effective Hamiltonian

$$K_2 = S_{d-1} \sum_{\Delta_{\mathcal{O}} < 2\Delta - d} \langle f | \, \mathcal{O}(1) \, | i \rangle \left(\lambda^{\mathcal{O}}_{\text{ren}} + \frac{g^2 f_{\phi\phi\mathcal{O}}}{2} \sum_{n=0}^{2n+\Delta \leq \Delta_T - \Delta_i} \frac{u_n^{2\Delta - \Delta_{\mathcal{O}}}}{2n + \Delta} \right) + \ldots \tag{13}$$

- Spectrum is finite as $\Delta_T \to \infty$ (at this order in PT).

Result at Second Order

Renormalized Effective Hamiltonian

$$K_2 = S_{d-1} \sum_{\Delta_{\mathcal{O}} < 2\Delta - d} \langle f | \, \mathcal{O}(1) \, | i \rangle \left(\lambda^{\mathcal{O}}_{\text{ren}} + \frac{g^2 f_{\phi\phi\mathcal{O}}}{2} \sum_{n=0}^{2n+\Delta \le \Delta_T - \Delta_i} \frac{u_n^{2\Delta - \Delta_{\mathcal{O}}}}{2n + \Delta} \right) + \dots \tag{13}$$

- Spectrum is finite as $\Delta_T \to \infty$ (at this order in PT).
- Although individual matrix elements blow up as $\Delta_T \to \infty$.

Result at Second Order

Renormalized Effective Hamiltonian

$$K_2 = S_{d-1} \sum_{\Delta_{\mathcal{O}} < 2\Delta - d} \langle f | \, \mathcal{O}(1) \, | i \rangle \left(\lambda^{\mathcal{O}}_{\text{ren}} + \frac{g^2 f_{\phi\phi\mathcal{O}}}{2} \sum_{n=0}^{2n+\Delta \leq \Delta_T - \Delta_i} \frac{u_n^{2\Delta - \Delta_{\mathcal{O}}}}{2n + \Delta} \right) + \dots \tag{13}$$

- Spectrum is finite as $\Delta_T \to \infty$ (at this order in PT).
- Although individual matrix elements blow up as $\Delta_T \to \infty$.
- K_2 is a *nonlocal* interaction.

Result at Second Order

Renormalized Effective Hamiltonian

$$K_2 = S_{d-1} \sum_{\Delta_{\mathcal{O}} < 2\Delta - d} \langle f | \mathcal{O}(1) | i \rangle \left(\lambda^{\mathcal{O}}_{\text{ren}} + \frac{g^2 f_{\phi\phi\mathcal{O}}}{2} \sum_{n=0}^{2n+\Delta \leq \Delta_T - \Delta_i} \frac{u_n^{2\Delta - \Delta_{\mathcal{O}}}}{2n+\Delta} \right) + \dots \tag{13}$$

- Spectrum is finite as $\Delta_T \to \infty$ (at this order in PT).
- Although individual matrix elements blow up as $\Delta_T \to \infty$.
- K_2 is a *nonlocal* interaction.
- Adding K_2 will affect energy differences between states.

Result at Second Order

Renormalized Effective Hamiltonian

$$K_2 = S_{d-1} \sum_{\Delta_{\mathcal{O}} < 2\Delta - d} \langle f | \, \mathcal{O}(1) \, | i \rangle \left(\lambda^{\mathcal{O}}_{\text{ren}} + \frac{g^2 f_{\phi\phi\mathcal{O}}}{2} \sum_{n=0}^{2n+\Delta \leq \Delta_T - \Delta_i} \frac{u_n^{2\Delta - \Delta_{\mathcal{O}}}}{2n + \Delta} \right) + \ldots \tag{13}$$

- Spectrum is finite as $\Delta_T \to \infty$ (at this order in PT).
- Although individual matrix elements blow up as $\Delta_T \to \infty$.
- K_2 is a *nonlocal* interaction.
- Adding K_2 will affect energy differences between states.
- We have also calculated K_3 using this methodology.

Example I: Ising $+ \epsilon$

A simple, well studied example QFT with UV divergences is the 2d Ising CFT deformed with its ϵ operator.

$$H = H_{\text{CFT}}^{\text{Ising}} + \frac{m}{2\pi} \int_0^{2\pi R} dx\, \epsilon(0, x)\,. \tag{14}$$

This QFT is actually the free massive fermion in disguise.

Example I: Ising $+\ \epsilon$

A simple, well studied example QFT with UV divergences is the 2d Ising CFT deformed with its ϵ operator.

$$H = H_{\text{CFT}}^{\text{Ising}} + \frac{m}{2\pi} \int_0^{2\pi R} dx\, \epsilon(0,x)\,. \tag{14}$$

This QFT is actually the free massive fermion in disguise.

Naively, this QFT has a UV divergence when the mass is added as a deformation:

$$E_{gs} \sim m^2 \log\left(R\Lambda_{UV}\right)$$

CFT Hamiltonian

The CFT Hamiltonian is the dilatation operator, Weyl transformed to the cylinder

$$H_{\text{CFT}}^{\text{Ising}} = \frac{1}{R}\left(D - \frac{c}{12}\right) \tag{15}$$

Its eigenstates are built systematically by acting on the vacuum with primary operators $\phi_p = \{\mathbb{1}, \sigma, \epsilon\}$ and Virasoro generators:

$$|\psi\rangle = L_{-n_1} \dots L_{-n_k} \bar{L}_{-m_1} \dots \bar{L}_{-m_l}\, \phi_p(0,0)\, |0\rangle \tag{16}$$

Renormalization

To deal with the UV divergence in the ground state energy, we follow our procedure from section IV and first add the only local counterterm we need:

$$H_{ct}(\delta) = \lambda_{ct}^{\mathbb{1}}(\delta) \int_0^{2\pi R} dx\, \mathbb{1}\,, \tag{17}$$

We pick the scheme

$$\lambda_{\text{ct}}^{\mathbb{1}}(\delta) = \frac{m^2}{4\pi^2} \int\limits_{\substack{0\leq|x|<1 \\ 1>|1-x|>\delta}} \frac{d^2x}{|x|} \langle \epsilon(1)\epsilon(x)\rangle\,, \tag{18}$$

so that

$$K_2 = \langle f|\, i\rangle\, m^2 R \sum_{n=0}^{2n+1\leq\Delta_T-\Delta_i} \frac{1}{2n+1} \tag{19}$$

Spectrum

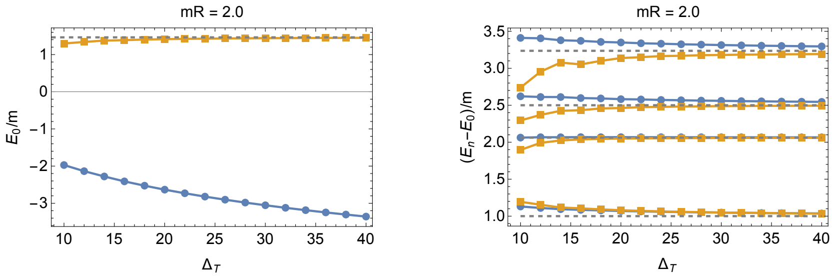

Figure: Plots indicating the variation of estimates for the Ising + ϵ spectrum with the truncation parameter Δ_T. The raw Hamiltonian is shown in blue and the estimate using K_2 is shown in orange. Exact results for this soluble QFT are plotted as gray dashed lines.

$\Delta_T = 40$ corresponds to a truncated Hilbert space with $\sim 22,000$ states

Variation with m

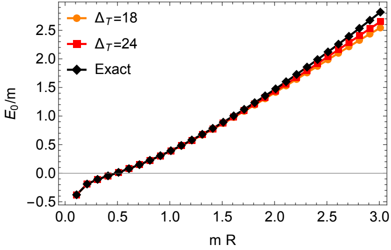

Figure: Comparison between results for the ground state energy using the renormalized effective Hamiltonian and the exact answer.

$$E_0(R) = -\frac{m^2 R}{4}\left(1 - \log(2m^2R^2) - 2\gamma\right) \\ - |m| \int_{-\infty}^{\infty} \frac{d\theta}{2\pi} \cosh\theta \log\left(1 + e^{-2\pi|m|R\cosh\theta}\right) . \quad (20)$$

Example II: Tricritical Ising + ϵ'

The ϵ' operator triggers an RG flow from the 2d Tricritical Ising CFT to the Ising CFT

$$H = H_{\text{CFT}}^{\text{Tricritical}} + \frac{g}{2\pi} \int_0^{2\pi R} dx \, \epsilon'(0, x) \,. \tag{21}$$

This flow has been studied before using TBA e.g [Zamolodchikov '91]and TCSA methods [Cardy, Lassig, Mussardo '90], [Giokas, Watts '11]

The ground state energy is more strongly UV divergent

$$E_{gs} \sim g^2 (R\Lambda_{UV})^{2/5} \,,$$

but there are no divergences at higher orders in perturbation theory.

Renormalization and the Effective Hamiltonian

Again, we need to introduce the local counterterm

$$H_{ct}(\delta) = \lambda^{\mathbb{1}}_{ct}(\delta) \int_0^{2\pi R} dx \, \mathbb{1} \,, \tag{22}$$

and pick the scheme

$$\lambda^{\mathbb{1}}_{\text{ct}}(\delta) = \frac{g^2}{4\pi^2} \int\limits_{\substack{0 \le |x| < 1 \\ 1 > |1-x| > \delta}} \frac{d^2 x}{|x|^{4/5}} \, \langle \epsilon'(1) \epsilon'(x) \rangle \,, \tag{23}$$

This time, we use both the $\mathbb{1}$ and ϵ' terms in $H_{\text{eff } 2}$ and also the $\mathbb{1}$ term in $H_{\text{eff } 3}$. The last two are “improvement terms”. They vanish and have no effect in the $\Delta_T \to \infty$ limit, but they improve the rate of convergence of results with Δ_T.

Spectrum

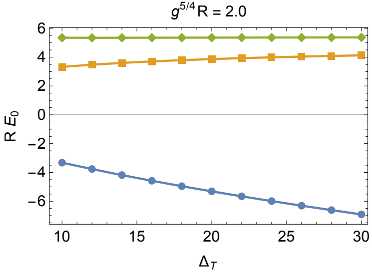

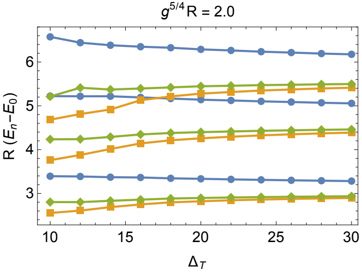

Figure: Plots indicating the variation of estimates for the Tricritical Ising + ϵ' spectrum with the truncation parameter Δ_T. The raw Hamiltonian is shown in blue, the estimate using $K_{\text{eff }2}$ is shown in orange and the estimate using $K_{\text{eff }2} + K_{\text{eff }3}$ is shown in green.

Variation with g

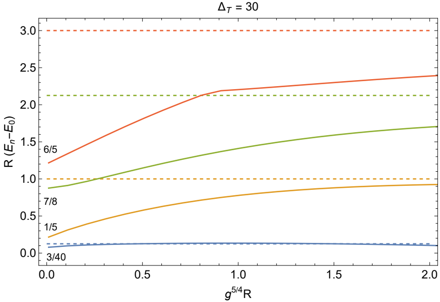

Figure: Four smallest energy gaps as function of radius, using $K_{\text{eff}\ 2,3}$ and $\Delta_T = 30$ with 40818 states total including all symmetry subsectors.

For large volumes, we find the spectrum approaches the Ising CFT:

$$E_i = \frac{\Delta_i}{R} + \Lambda^2 R\,. \tag{24}$$

Hamiltonian Truncation on NISQ Devices

Based on [2407.19022] with M. Spannowsky,
T. Sypchenko and S. Williams.

General Idea

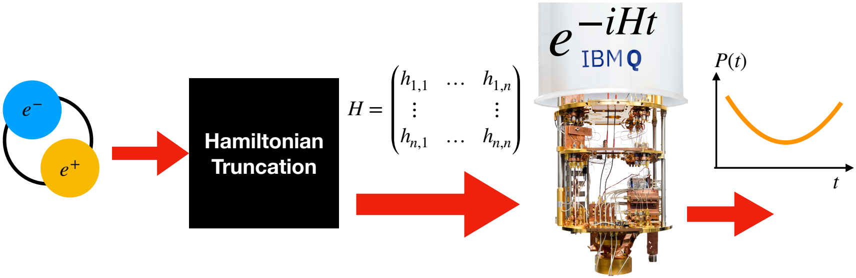

1. We compute the probability that the Schwinger Model QFT remains in its ground state following a quantum quench.

General Idea

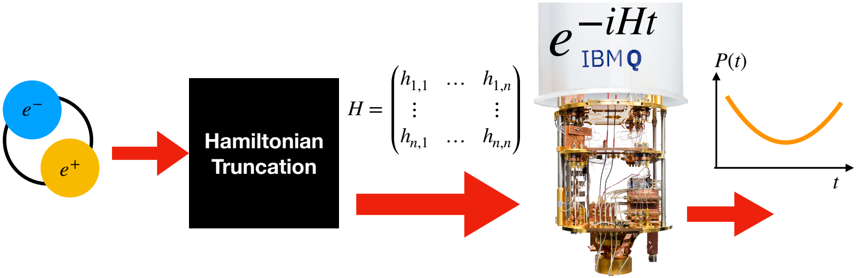

1. We compute the probability that the Schwinger Model QFT remains in its ground state following a quantum quench.
2. We use Hamiltonian Truncation to generate an approximate Hamiltonian for our system of low dimensionality.

General Idea

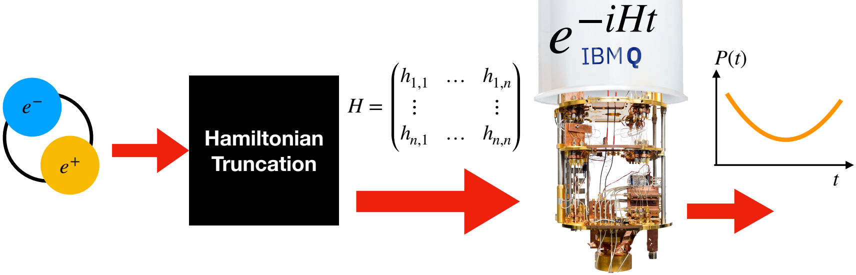

1. We compute the probability that the Schwinger Model QFT remains in its ground state following a quantum quench.
2. We use Hamiltonian Truncation to generate an approximate Hamiltonian for our system of low dimensionality.
3. We use a qubit based, gate based, quantum device from IBM to determine how this probability evolves with time.

Schwinger Model

QED in 1+1 dimensions

$$\mathcal{L} = -\frac{1}{4} F_{\mu\nu} F^{\mu\nu} + \bar{\psi} \left(i \not{\partial} - g \not{A} - m \right) \psi \, , \tag{25}$$

- Shares qualitative features with QCD including confinement, chiral symmetry breaking, $U(1)_A$ anomaly.
- We take there to be only 1 Dirac fermion.
- Put on a circle of circumference L and use periodic boundary conditions.
- Studied extensively using lattice gauge theory on a variety of quantum computing platforms e.g. [P. Hauke et al '13].

Bosonisation

The $m = 0$ theory was solved exactly by Schwinger. It is a theory of confined, noninteracting, pseudoscalar mesons.

$$H_0 = \frac{1}{2}\int_0^L dx \; :\Pi^2 + (\partial_x \phi)^2 + \frac{g^2}{\pi}\phi^2: \; , \tag{26}$$

The scalar has mass $M = g/\sqrt{\pi}$. Bosonisation helpfully removes gauge redundant d.o.fs. Normal ordering in (26) removes UV divergences.

Bosonisation

The $m = 0$ theory was solved exactly by Schwinger. It is a theory of confined, noninteracting, pseudoscalar mesons.

$$H_0 = \frac{1}{2}\int_0^L dx \ :\Pi^2 + (\partial_x\phi)^2 + \frac{g^2}{\pi}\phi^2: \ , \tag{26}$$

The scalar has mass $M = g/\sqrt{\pi}$. Bosonisation helpfully removes gauge redundant d.o.fs. Normal ordering in (26) removes UV divergences.

When $m \neq 0$, the theory becomes interacting

$$V = -2cmM\int_0^L dx \ :\cos\left(\sqrt{4\pi}\phi + \theta\right):, \tag{27}$$

chiral symmetry is broken, and the θ parameter becomes physical, but we only consider $\theta = 0$ here.

Basis States

Quantise the massive scalar field on the circle

$$\phi(x) = \sum_{n=-\infty}^{\infty} \frac{1}{\sqrt{2LE_n}} \left(a_n \, e^{ik_n x} + a_n^\dagger \, e^{-ik_n x} \right) \ . \tag{28}$$

where the n represent the different momentum modes on the circle $k_n = 2\pi n/L$.

Work in eigenbasis of H_0

$$|\{\mathbf{r}\}\rangle = \prod_{n=-\infty}^{n=\infty} \frac{1}{\sqrt{r_n!}} \left(a_n^\dagger \right)^{r_n} |0\rangle \ , \tag{29}$$

which is the usual Fock basis.

Truncation

List the states in order of increasing H_0 eigenvalue and take the first 2^{n_q} states from this list.

For instance, with $n_q = 2$ and $gL = 8$, the states we would retain are

$$|0\rangle\,, \quad \frac{1}{\sqrt{2}}\left(a_0^\dagger\right)^2|0\rangle\,, \quad a_1^\dagger a_{-1}^\dagger|0\rangle\,, \quad \frac{1}{\sqrt{4!}}\left(a_0^\dagger\right)^4|0\rangle\,. \tag{30}$$

These states form our computational basis for quantum computing. Calculate matrix elements

$$V_{\mathbf{r},\mathbf{r}'} = \left\langle\{\mathbf{r}'\}\right| :\cos\left(\sqrt{4\pi}\phi\right): \left|\{\mathbf{r}\}\right\rangle \tag{31}$$

between these states. Gives H as a $2^{n_q} \times 2^{nq}$ matrix

Sanity Check

Numerical estimates for particle masses converge to known results as (qubit number n_q) is increased

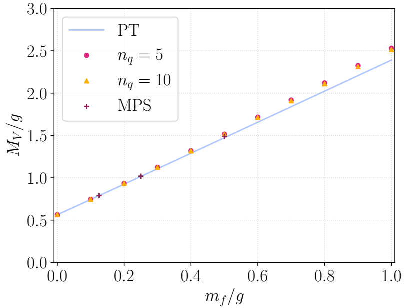

HT data taken at $gL = 8$. PT = second order perturbation theory in infinite volume. MPS = matrix product states M. Bañuls et al '13.

Quantum Quench

We consider the time dependence of the probability that the Schwinger model stays in its $m = 0$ vacuum state, following a quantum quench to $m/g = 0.2$.

$$G(t) = \left\langle 0 \middle| e^{-iHt} \middle| 0 \right\rangle \ , \qquad P(t) = |G(t)|^2 \,. \tag{32}$$

This particular probability cannot be computed without state preparation in Kogut-Susskind lattice formulation of the Schwinger model.

These routines can be extremely costly. The resources required to implement the state-preparation for an arbitrary state can scale exponentially [Sun et al '23].

Time Evolution Converges

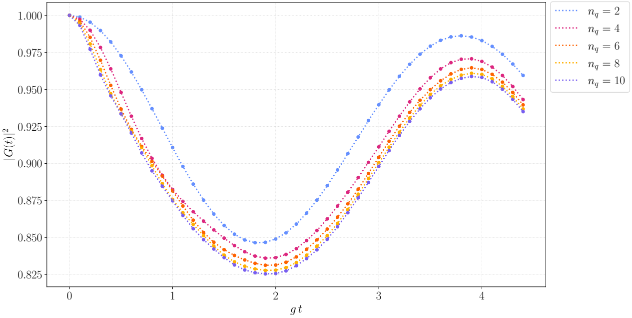

- The vacuum survival probability converges as $n_q \to \infty$.
- Already at $n_q = 2$, we get a reasonable approximation to the continuum time evolution. We are within 5% of the $n_q = 10$ result.
- This is a classical calculation.

Device Basics

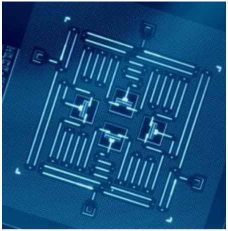

Figure: Image credit: [J. Gambetta et al '17]

Name	Function	Symbol	Matrix
Pauli-X (X)	$\hat{R}_x(\pi)$	$\boxed{X}$	$\begin{pmatrix} 0 & 1 \\ 1 & 0 \end{pmatrix}$
Pauli-Y (Y)	$\hat{R}_y(\pi)$	$\boxed{Y}$	$\begin{pmatrix} 0 & -\mathrm{i} \\ \mathrm{i} & 0 \end{pmatrix}$
Pauli-Z (Z)	$\hat{R}_z(\pi)$	$\boxed{Z}$	$\begin{pmatrix} 1 & 0 \\ 0 & -1 \end{pmatrix}$
Hadamard (H)	$\hat{R}_z(\pi)\hat{R}_x(\pi/2)$	$\boxed{H}$	$\frac{1}{\sqrt{2}}\begin{pmatrix} 1 & 1 \\ 1 & -1 \end{pmatrix}$
Phase (S)	$\hat{R}_z(\pi/2)$	$\boxed{S}$	$\begin{pmatrix} 1 & 0 \\ 0 & \mathrm{i} \end{pmatrix}$
$\pi/8$ (T)	$\hat{R}_z(\pi/4)$	$\boxed{T}$	$\begin{pmatrix} 1 & 0 \\ 0 & e^{\mathrm{i}\pi/4} \end{pmatrix}$
Controlled-NOT (CNOT)	$\hat{X}\,\lvert\psi\rangle_t$ if $\lvert\psi\rangle_c = \lvert 1\rangle$	$\bullet$ / $\oplus$	$\begin{pmatrix} 1 & 0 & 0 & 0 \\ 0 & 1 & 0 & 0 \\ 0 & 0 & 0 & 1 \\ 0 & 0 & 1 & 0 \end{pmatrix}$

Figure: Universal set of gates [S. Kwon et al '21]

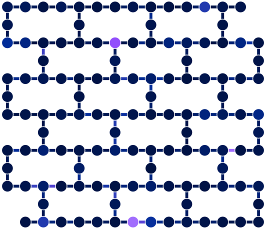

Figure: Connectivity of gates for `ibm_brisbane`

Pauli Decomposition

To do the calculation on a NISQ device, we decompose the Hamiltonian as

$$H = \sum_{i_1 \ldots i_{n_q} = 0}^{3} \alpha_{i_1 \ldots i_{n_q}} \left(\sigma_{i_1} \otimes \cdots \otimes \sigma_{i_{n_q}} \right) \tag{33}$$

Any Hermitian matrix can be decomposed this way to yield real coefficients $\alpha_{i_1 \ldots i_{n_q}}$.

For a generic dense Hamiltonian matrix, there will be $\sim 4^{n_q}$ nonzero coefficients in this decomposition.

Trotterisation

We use the Trotter-Suzuki approximation to first order. Error $\sim O(t^2/n)$.

$$|\psi(t)\rangle = e^{-iHt}|\psi(0)\rangle \approx \left[\prod_{i_1,\ldots,i_{n_q}} e^{-i\frac{t}{n}\alpha_{i_1,\ldots,i_{n_q}}\left(\sigma_{i_1}\otimes\cdots\otimes\sigma_{i_{n_q}}\right)}\right]^n |\psi(0)\rangle \ . \quad (34)$$

The exponential of each Pauli term can be implemented on a qubit-based quantum device through a *short* sequence of single-qubit rotation gates and CNOT gates.

Trotter Error

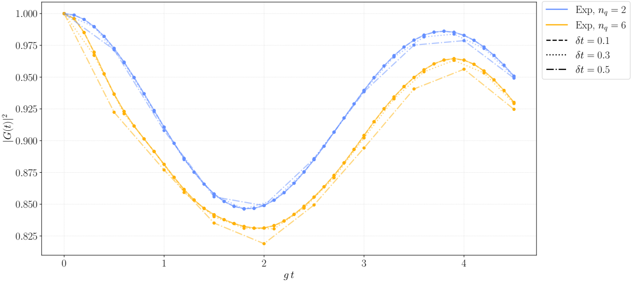

Figure: Blue curves are for $n_q = 2$ and yellow for $n_q = 6$.

We will use $gt/n = g\delta t = 0.3$ for $n_q = 2$ on the quantum device.

Quantum Hamiltonian Truncation

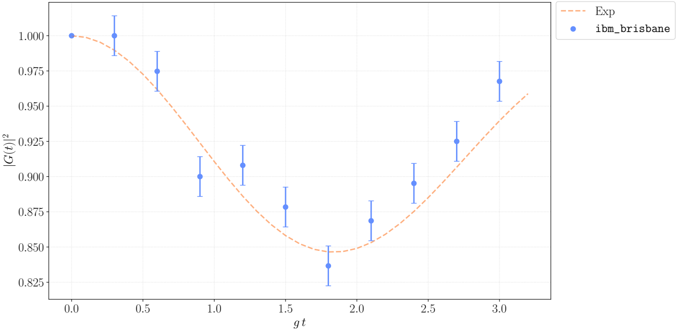

Figure: Time evolution of the Schwinger model via HT run on the ibm brisbane 127-qubit quantum computer (though we only use 2 of them). The results are enhanced using error mitigation and suppression routines through QISKIT and Q-CTRL.

Summary and Conclusion I

1. Hamiltonian Truncation (HT) is a framework for extracting predictions from quantum theories non-perturbatively.

Summary and Conclusion I

1. Hamiltonian Truncation (HT) is a framework for extracting predictions from quantum theories non-perturbatively.
2. The TCSA is HT applied to QFTs defined as a CFT deformed with relevant operators on the cylinder.

Summary and Conclusion I

1. Hamiltonian Truncation (HT) is a framework for extracting predictions from quantum theories non-perturbatively.
2. The TCSA is HT applied to QFTs defined as a CFT deformed with relevant operators on the cylinder.
3. For QFTs with UV divergences, nonlocal Δ_T divergent interactions must be added to the truncated Hamiltonian.

Summary and Conclusion I

1. Hamiltonian Truncation (HT) is a framework for extracting predictions from quantum theories non-perturbatively.
2. The TCSA is HT applied to QFTs defined as a CFT deformed with relevant operators on the cylinder.
3. For QFTs with UV divergences, nonlocal Δ_T divergent interactions must be added to the truncated Hamiltonian.
4. We have shown how to calculate the required nonlocal interactions in TCSA, using an effective Hamiltonian.

Summary and Conclusion I

1. Hamiltonian Truncation (HT) is a framework for extracting predictions from quantum theories non-perturbatively.
2. The TCSA is HT applied to QFTs defined as a CFT deformed with relevant operators on the cylinder.
3. For QFTs with UV divergences, nonlocal Δ_T divergent interactions must be added to the truncated Hamiltonian.
4. We have shown how to calculate the required nonlocal interactions in TCSA, using an effective Hamiltonian.
5. We demonstrate the viability of using HT to facilitate the non-perturbative, real-time simulation of QFTs on NISQ devices.

Summary and Conclusion I

1. Hamiltonian Truncation (HT) is a framework for extracting predictions from quantum theories non-perturbatively.
2. The TCSA is HT applied to QFTs defined as a CFT deformed with relevant operators on the cylinder.
3. For QFTs with UV divergences, nonlocal Δ_T divergent interactions must be added to the truncated Hamiltonian.
4. We have shown how to calculate the required nonlocal interactions in TCSA, using an effective Hamiltonian.
5. We demonstrate the viability of using HT to facilitate the non-perturbative, real-time simulation of QFTs on NISQ devices.
6. The tools we used could be applied to many other QFTs and observables - there are many other exciting applications to explore!

Thank you!

The Schrieffer–Wolff Effective Hamiltonian

The Schrieffer–Wolff Hamiltonian [Schrieffer, Wolff '66] has the properties we need to play the role of an effective Hamiltonian:

$$H_{\text{eff}}^{SW} = \left[e^{S}\left(H_0 + gV\right)e^{-S}\right]_l \,, \tag{35}$$

e^S is a canonical transformation constructed to block diagonalize the full theory Hamiltonian order by order in PT:

$$e^{S}\left(H_0 + gV\right)e^{-S} = \begin{pmatrix} H_{\text{eff}}^{SW} & 0 \\ 0 & H_{hh} \end{pmatrix} .$$

The sizes of the blocks may be freely chosen. Choose the block size so that H_{eff}^{SW} only acts on states $E_i \leq \Delta_T/R$:

S is constructed to be anti–hermitian, so H_{eff}^{SW} *is* hermitian.

Truncation

e^S is unitary: Spectrum of H_{eff}^{SW} exactly matches low energy spectrum of the full theory:

Finally, we truncate the Hilbert space, so that only states with $E_i \leq \Delta_T/R$ are retained:

$$\begin{pmatrix} \boxed{\begin{matrix} 1 & 3 \\ 3 & 2 \end{matrix}} & \begin{matrix} 0 & 0 \\ 0 & 0 \end{matrix} & \cdots \\ \begin{matrix} 0 & 0 \\ 0 & 0 \end{matrix} & \begin{matrix} 12 & 7 \\ 7 & -6 \end{matrix} & \\ \vdots & & \ddots \end{pmatrix} \Longrightarrow \begin{pmatrix} 1 & 3 \\ 3 & 2 \end{pmatrix}$$

Expanding H_{eff} in Perturbation Theory

$$\left(H^{SW}_{\text{eff}\,2}\right)_{fi} = \frac{1}{2}\left(\frac{V_{fh}V_{hi}}{E_{fh}} + \frac{V_{fh}V_{hi}}{E_{ih}}\right), \tag{36}$$

$$\left(H^{SW}_{\text{eff}\,3}\right)_{fi} = \frac{1}{2}\left(\frac{V_{fh_1}V_{h_1h_2}V_{h_2i}}{E_{fh_1}E_{fh_2}} - \frac{V_{fl}V_{lh}V_{hi}}{E_{fh}E_{lh}} + \text{h.c.}\right), \tag{37}$$

- Repeated h_i indices denote sums over states above the cutoff.
- Repeated l_i indices denote sums over states in the truncated Hilbert space.
- Higher order corrections suppressed by $\sim V_{ij}/(E_h - E_i)$. Denominator is large for states with energy much lower than cutoff.

Fourth Order

$$
\begin{aligned}
\left(H^{SW}_{\text{eff }4}\right)_{fi} = &-\frac{1}{2}\frac{V_{fh_1}V_{h_1h_2}V_{h_2h_3}V_{h_3i}}{E_{h1f}E_{h2f}E_{h3f}} + \frac{1}{2}\frac{V_{fh_1}V_{h_1h_2}V_{h_2l_1}V_{l_1i}}{E_{h_1i}E_{h_1l_1}E_{h_2l_1}} \\
&+ \frac{1}{2}\frac{V_{fh_1}V_{h_1h_2}V_{h_2l_1}V_{l_1i}}{E_{h_1i}E_{h_2i}E_{h_1l_1}} - \frac{1}{2}\frac{V_{fh_1}V_{h_1l_1}V_{l_1l_2}V_{l_2i}}{E_{h_1i}E_{h_1l_1}E_{h_1l_2}} \\
&+ \frac{1}{3!}\frac{V_{fh_1}V_{h_1l_1}V_{l_1h_2}V_{h_2i}}{E_{h_1f}E_{h_2f}E_{h_1l_1}} + \frac{2}{3!}\frac{V_{fh_1}V_{h_1l_1}V_{l_1h_2}V_{h_2i}}{E_{h_1f}E_{h_2f}E_{h_2l_1}} + \frac{1}{3!}\frac{V_{fh_1}V_{h_1l_1}V_{l_1h_2}V_{h_2i}}{E_{h_2f}E_{h_1l_1}E_{h_2l_1}} \\
&- \frac{1}{4!}\frac{V_{fh_1}V_{h_1l_1}V_{l_1h_2}V_{h_2i}}{E_{h_1f}E_{h_2l_1}E_{h_1l_1}} - \frac{3}{4!}\frac{V_{fh_1}V_{h_1l_1}V_{l_1h_2}V_{h_2i}}{E_{h_1f}E_{h_1l_1}E_{h_2i}} + \text{h.c.} \qquad (38)
\end{aligned}
$$

Alternative Effective Hamiltonians

In [Cohen, Farnsworth, Houtz, Luty '21], another effective Hamiltonian was introduced, which can also be written as

$$H_{\text{eff}} = (\Sigma_l)^{-1} \left[\Sigma (H_0 + V) \Sigma^\dagger \right]_l \Sigma_l \,, \tag{39}$$

where Σ is given by

$$\Sigma = \lim_{t_f \to \infty} U_{\text{IP}}(t_f, 0) \,. \tag{40}$$

In scattering theory, it is often called Møller operator.

Effective Hamiltonian in PT

When expanded in perturbation theory, it has a more compact form

$$(H_{\text{eff}\,2})_{fi} = \frac{V_{fh} V_{hi}}{E_{fh}}, \tag{41}$$

$$(H_{\text{eff}\,3})_{fi} = \frac{V_{fh_1} V_{h_1 h_2} V_{h_2 i}}{E_{fh_1} E_{fh_2}} - \frac{V_{fl} V_{lh} V_{hi}}{E_{fh} E_{lh}}, \tag{42}$$

$$\begin{aligned}(H_{\text{eff}\,4})_{fi} = &\frac{V_{fh_1} V_{h_1 h_2} V_{h_2 h_3} V_{h_3 i}}{E_{fh_1} E_{fh_2} E_{fh_3}} - \frac{V_{fh_1} V_{h_1 l} V_{lh_2} V_{h_2 i}}{E_{fh_1} E_{fh_2} E_{lh_2}} \\ &- \frac{V_{fl} V_{lh_1} V_{h_1 h_2} V_{h_2 i}}{E_{fh_1} E_{lh_2}} \left[\frac{1}{E_{fh_2}} + \frac{1}{E_{lh_1}} \right] + \frac{V_{fl_1} V_{l_1 l_2} V_{l_2 h} V_{hi}}{E_{fh} E_{l_1 h} E_{l_2 h}},\end{aligned} \tag{43}$$

although it is non-hermitian.